



RESEARCH LETTER

10.1002/2017GL074934

Key Points:

- Large earthquakes are synchronized
- Therefore, the likelihood of earthquakes with particular characteristics varies in time in a quantifiable way
- Changes in length of day can excite sets of earthquakes with short renewal intervals

Supporting Information:

- Supporting Information S1

Correspondence to:

R. Bendick,
bendick@mso.umt.edu

Citation:

Bendick, R., and R. Bilham (2017), Do weak global stresses synchronize earthquakes?, *Geophys. Res. Lett.*, *44*, 8320–8327, doi:10.1002/2017GL074934.

Received 8 JUN 2017

Accepted 11 AUG 2017

Accepted article online 16 AUG 2017

Published online 26 AUG 2017

Do weak global stresses synchronize earthquakes?

R. Bendick¹  and R. Bilham² ¹University of Montana, Missoula, Montana, USA, ²CIRES, University of Colorado, Boulder, Colorado, USA

Abstract Insofar as slip in an earthquake is related to the strain accumulated near a fault since a previous earthquake, and this process repeats many times, the earthquake cycle approximates an autonomous oscillator. Its asymmetric slow accumulation of strain and rapid release is quite unlike the harmonic motion of a pendulum and need not be time predictable, but still resembles a class of repeating systems known as integrate-and-fire oscillators, whose behavior has been shown to demonstrate a remarkable ability to synchronize to either external or self-organized forcing. Given sufficient time and even very weak physical coupling, the phases of sets of such oscillators, with similar though not necessarily identical period, approach each other. Topological and time series analyses presented here demonstrate that earthquakes worldwide show evidence of such synchronization. Though numerous studies demonstrate that the composite temporal distribution of major earthquakes in the instrumental record is indistinguishable from random, the additional consideration of event renewal interval serves to identify earthquake groupings suggestive of synchronization that are absent in synthetic catalogs. We envisage the weak forces responsible for clustering originate from lithospheric strain induced by seismicity itself, by finite strains over teleseismic distances, or by other sources of lithospheric loading such as Earth's variable rotation. For example, quasi-periodic maxima in rotational deceleration are accompanied by increased global seismicity at multidecadal intervals.

Plain Language Summary Large earthquakes appear to synchronize globally, in the sense that they are organized in time according to their renewal properties, and occur in groups in response to very low stress interactions.

1. Introduction

Synchronized systems are those in which self-sustained oscillators, which may be noisy or even chaotic, systematically approach phase coherence in the presence of weak coupling. The presence of such synchronization in a system of many oscillators does not always permit a controlling mechanism to be quantified since the weak forces influencing the ensemble system are often close to, or below, system noise [Oliveira and Melo, 2015; Winfree, 1967]. The phenomenon of synchronization has been reported in weakly coupled mechanical, biological, and chemical systems, ranging from the relatively simple, such as Huygen's clocks [Czolczynski et al., 2009; Oliveira and Melo, 2015] and celestial orbits, to the complex, such as firefly lighting, neuron firing [Mirrollo and Strogatz, 1990], and regional [Scholz, 2010] and simulated [Sammis and Smith, 2013] seismicity.

When such systems contain large numbers of oscillators, the coupling is weak, or the oscillators are themselves noisy (i.e., their period is imperfect), the state of synchronization itself may also be noisy, with individual or sets of oscillators shifting out of phase for some cycles [Pikovsky et al., 2003; Kuramoto and Battogtokh, 2002] and stable or quasi-stable subsets of in-phase oscillators not synchronized to each other. Furthermore, when the natural periods of oscillators differ, that is, the oscillators have different mechanical properties [Daido, 1995; Okuda, 1993] or the coupling mechanism attenuates with distance [Leyva et al., 2011], limited subsets of the whole population are expected to be synchronized at any particular time interval [Kuramoto and Battogtokh, 2002], and both spatial and temporal synchronization waves may travel through the system [Leyva et al., 2011].

Regardless of such complications, the fundamental prerequisites for synchronization are merely that a system is made of many oscillatory elements, that these elements are quasi-periodic, and that the individual elements are open, so that they may interact with other elements. In mechanical versions of such systems, such as simple pendulums in proximity, synchronization arises over many cycles during which weak interactions nudge the phase of all oscillators into phase coherence; in earthquakes this nudging is manifest through clock advances or delays [Scholz, 2010]. Such synchronization differs from direct triggering in that the

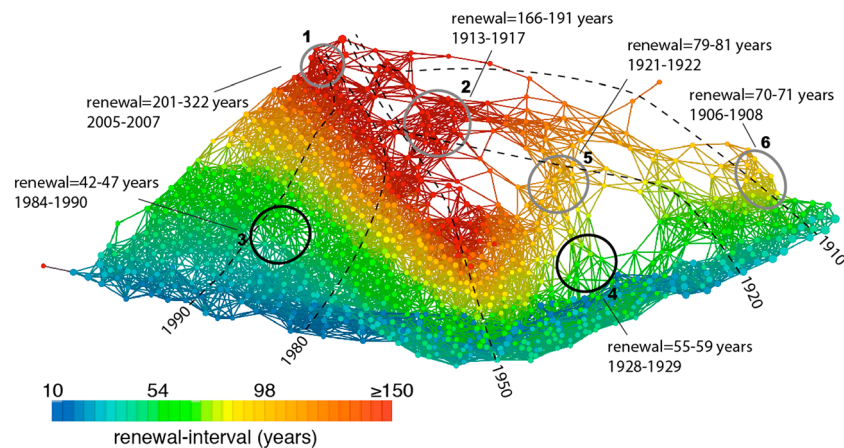


Figure 1. A topological network [Carlsson, 2009] relating earthquakes (nodes) with similar renewal interval and date of occurrence using a variance-normalized Euclidian metric on two real-valued derived measures of event properties: L-infinity centrality and Gaussian density. See text for discussion. Nodes contain sets of events similar in timing and renewal interval, connected based on events common to sets. The length of links between nodes is proportional to the similarity of the properties of the linked nodes. Of interest in this topology are isolated clusters that are absent in the topology of random catalogs (see supporting information). The properties of several prominent clusters are itemized, with the values giving the range of the central quintile. Earthquake dates are contoured with dashed lines, and renewal intervals are color coded (saturated for intervals ≥ 150 years). Node diameter is proportional to the number of events combined in a single node. Bold numbers are cluster numbering used in the extended data. The largest cluster (1) contains 44 events, the smallest (3 and 4) contain 20 events. The pair of black circles identify a repeating cluster with a ≈ 50 year renewal interval. Circled clusters are representative examples; the topological network contains additional features not discussed in the analysis.

forcing is much smaller and in the absence of weak interaction, the oscillators would manifest their dynamic motion in isolation, but with arbitrary phase. The temporal evolution of synchronization involves propagation of phase from sets of neighbors with the closest natural frequencies, and has been described by the Kuramoto phase transition [Kuramoto, 1975]. Clusters of oscillators can merge or stably coexist. The “size” of synchronized clusters (i.e., how many oscillators therein) is determined by tradeoffs between the coupling, the frequency range of members, and the attenuation of coupling such that if the coupling is large, then oscillators with a wider range of natural frequencies and over greater distances are synchronized [Pikovsky et al., 2003].

Synchronization phenomena may be expected regardless of whether oscillators behave as chaotic oscillators [Wang et al., 2000], noisy and incompletely coupled oscillators [Daido, 1995; Acebron et al., 1998], or integrate-and-fire oscillators [Mirollo and Strogatz, 1990; Prignano et al., 2012]. The last most resembles the earthquake cycle [Barbot et al., 2012; Dietrich, 1992] in that during the interseismic period (the renewal interval) elastic energy is stored near a fault which is partly or completely released during an earthquake [Rundle et al., 2002], and which may host events of many different sizes depending on the charging period. Scholz [2010] proposes “fuzzy” synchronization of such fault segments over regional distances through direct triggering. Sammis and Smith [2013] extend the concept to global distances for simulated perfectly periodic events. Both models note that event period determined by fault slip rates or recurrence intervals are critical parameters for determining synchronization.

We therefore search for statistical evidence of phase or period coherence in the occurrence of $M_w \geq 7$ earthquakes globally since 1900 (including known aftershocks and foreshocks) explicitly incorporating information about fault charging period. Because synchronization is expected at all scales [Leyva et al., 2011], any magnitude threshold could have been selected; however, the catalog becomes less and less complete for decreasing magnitudes [Shearer and Stark, 2012; Michael, 2014]. Our analyses focus on three parameters: the date of the earthquake, the elapsed *interevent-interval* between any two earthquakes in the catalog (independent of magnitude or location), and the *renewal interval* of individual earthquakes calculated from the slip in that earthquake and the local strain accumulation rate. We use these event properties rather than recurrence interval because they do not assume either slip-predictability or time-predictability of the earthquake “cycle.” This last parameter serves as a proxy for the charging interval of a particular fault segment. Although previous

studies have used many different statistical approaches to test for temporal clustering in global earthquake catalogs [e.g., *Shearer and Stark, 2012; Beroza, 2012; Ben-Naim et al., 2013; Daub et al., 2015*], none takes into account the necessary synchronization constraint that clusters should have structure related to both renewal interval and timing. Without accounting for the renewal interval dependence, the superposition of many different sets of synchronized events in any particular time interval means that the whole catalog approaches a homogeneous Poisson process [*Shearer and Stark, 2012*].

2. Methods

We use the geographically partitioned data base of *Berryman et al. [2015]*, which is partly based on the Centennial catalog [*Engdahl and Villaseñor, 2002*] (<https://earthquake.usgs.gov/data/centennial/>), supplemented by $M \geq 7$ earthquakes from the U.S. Geological Survey/National Earthquake Information Center catalog to 1 January 2017. *Bragato and Sagan [2014]* consider the Centennial Catalog to be complete to $M_w 7.0$ except for brief intervals prior to 1918. Catalog completeness for pre-1920 earthquakes is known to be an issue and is discussed by *Michael [2014]*. We consider our catalog to be complete for $M_w \geq 7.1$ for the period 1900–2017 (Table S1). The International Seismological Centre (ISC)/Global Earthquake Model (GEM) [*DiGiacomo et al., 2015*] is not used since it is acknowledged by ISC to be currently incomplete prior to 1917. We test for sensitivity to catalog completeness by running the same analyses on alternative event catalogs from different sources, with different start dates, with different magnitude cutoffs, with stochastic decimation, and with declustering to remove aftershocks (see supporting information). We do not treat aftershocks differently from main shocks in the primary analyses; they do not preferentially cluster with main shocks in the topological approach (Figure 2) because of their difference in magnitude; thus, renewal interval (see Figure S1) nor do aftershocks substantially change the prevalence of particular interevent intervals in the catalogs after declustering [*Reasenburg, 1985*].

A renewal interval for each earthquake is calculated using a semiempirical relation between event magnitude and mean slip using the scaling relationship given by *Leonard [2010]*, divided by the product of the local tectonic loading rate determined from the REVEL global plate motion model [*Sella et al., 2002*] and a local value for seismic coupling (the ratio of seismic to aseismic slip) derived by *Berryman et al. [2015]*. For the small number of events not located on a known plate boundary, the geodetically determined relative velocity across the event region was used instead, although we recognize this may be a poor proxy for renewal interval for these events [*Calais et al., 2016*]. Coupling coefficients are determined from a globally consistent method incorporating interface morphology, seismic moment release rates, and geodetic observations. The challenges inherent in assigning seismic coupling coefficients to tectonic boundaries in the absence of complete seismic catalogs is illustrated by differences between the *Berryman et al. [2015]* coupling values and those reported in *Scholz and Campos [2012]* using a different approach and a subset of data; in using *Berryman et al. [2015]* we ensure that estimates are consistently evaluated for the entire catalog. For events not on subduction boundaries, we use coupling coefficients derived from the regional literature where possible, such as in the Himalaya, or assign perfect coupling (coupling coefficient = 1.0) where no other information is available. Because the parameters used to calculate renewal interval are themselves based on a wide variety of data types and qualities, the renewal interval used in this study may not represent the actual renewal interval, much less the “true” natural period of a fault. However, these renewal intervals are intended to be consistently proportional to the natural frequency of the event, insofar as events with long calculated renewal times should be less frequent than those with short calculated renewal times. Because real faults host a wide range of event magnitudes, we recognize that these renewal intervals do not fully represent the richness of fault behavior and therefore underestimate the noisiness or stochasticity of faults as oscillators. The primary consequences are that clusters based on single interevent interval values are likely to be less stable than predicted by theory, and that fault patches may be members of many different clusters with different timing and renewal interval properties.

We first use topological data analysis (TDA) tools [*Carlsson, 2009*] to search simultaneously for patterns in the timing of events (from their date of occurrence) and their “natural frequency” (the calculated renewal interval parameter). These methods are optimized for pattern recognition in noisy and incomplete data; in particular, they identify subgroups in complex data [*Lum et al., 2013*]. The TDA approach provides a summary of the arrangement of events under all possible values of a distance parameter, in which distance is a measure of

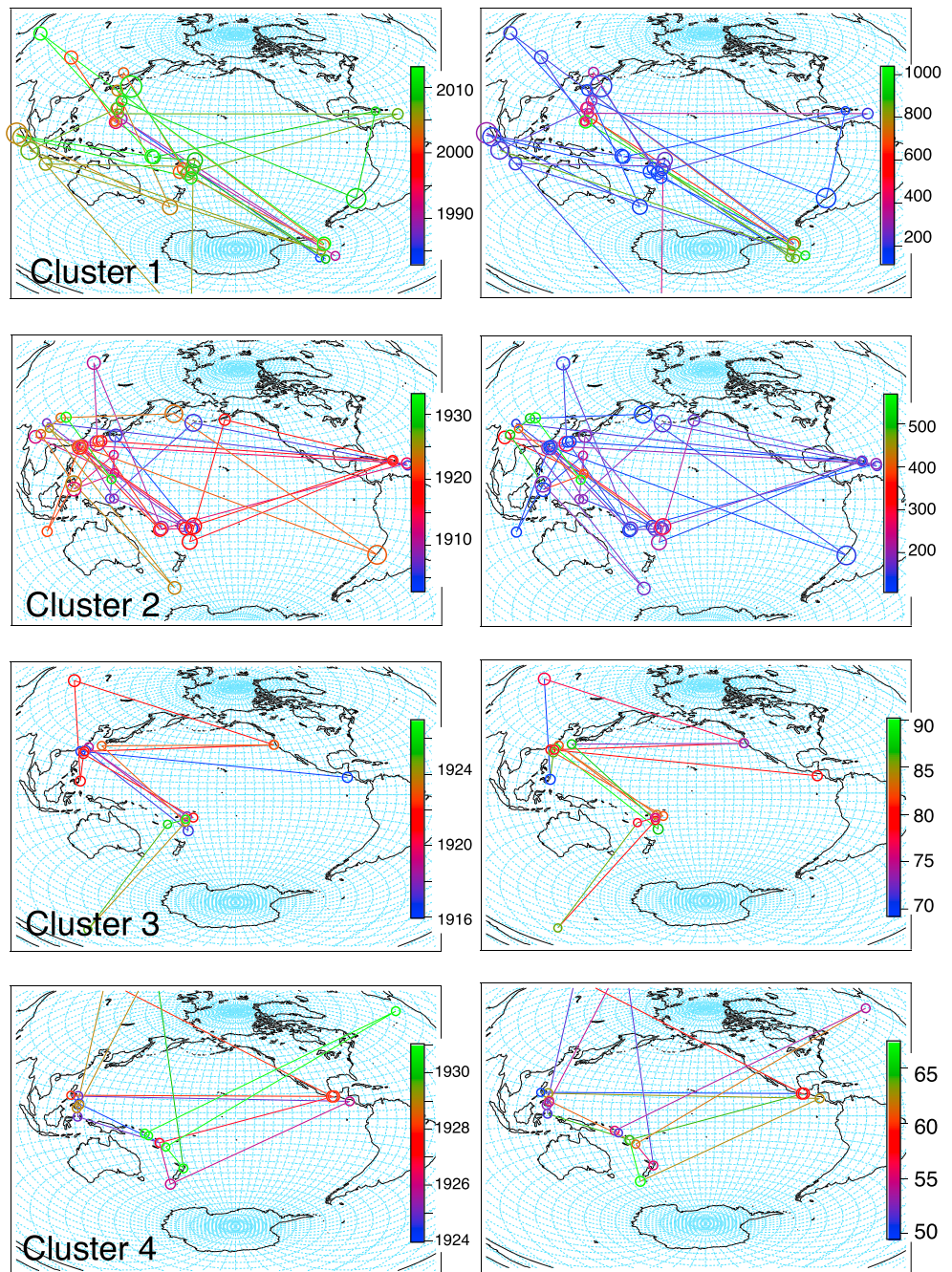


Figure 2. Maps of event location and timing for four of the six clusters identified in Figure 1 illustrate their global distribution. (left) Occurrence date versus location, (right), for the same clusters, renewal interval (years) versus location. The other two cluster maps are shown in figure ED2.

how alike event records are for any number of parameters. The length of the connections between nodes is therefore paramount, and the topological approach means that these connections are insensitive to scale, rotation, or other homogeneous transformations of the data (such as a choice of a different method of calculating renewal interval). As a result, groupings of points in the resulting network as in Figure 1 demonstrate that there exist sets of events in the catalog that are similar to one another with respect to both timing and renewal, but different from the other events in the catalog or the catalog mean, as quantified in Table S1, The TDA implemented in Ayasdi (www.ayasdi.com, Menlo Park, CA) requires a metric and a set of functions, called lenses, that map data to a real valued vector space [Singh *et al.*, 2007].

In the preferred analysis, we use the variance normalized Euclidian metric on L-infinity centrality and Gaussian density lenses. The graphical network thus consists of nodes representing sets of events with similar timing and renewal intervals and lines (edges) connecting nodes that contain events in common, with the length of the edges inversely proportional to the number of common events, hence representative of similarity. We compare the topological structure of the natural event catalog to 10 synthetic catalogs derived from the natural catalog by retaining event properties, including renewal interval, but randomizing the event times. The randomized catalogs treat aftershocks as independent events. The nonparametric Kolmogorov-Smirnov (KS) statistic is used to quantify the significance of clustering by comparing the probability distributions of events within a given cluster to those for all events not in the cluster, with higher KS scores indicating greater significance.

3. Results

The TDA reveals patterns in renewal interval and date (Figure 1). Topological mapping of these properties accentuates close groupings of events with similar renewal interval and timing. “Clusters” of nodes are therefore of particular interest because they include sets of earthquakes with similar renewal interval and date range, distinctly different from more distant nodes of earthquakes with different dates and/or renewal intervals. Clusters do not contain events that are spatially adjacent, as might be expected with direct triggering (Figures 2 and S3) or a strong role for aftershocks in determining topology. Clusters are particularly prominent for earthquakes with renewal intervals exceeding the 115 year duration of the catalog. Earthquakes with renewal intervals shorter than the catalog also cluster but appear to do so in sets with offset phase, as discussed below. Such clusters are notably absent in random number catalogs that we have simulated and subjected to identical analyses (Figure S2 and Table S1). The existence of prominent clusters with both common date and renewal interval should not occur if random processes prevail in the earthquake catalog [Shearer and Stark, 2012]. The properties of a number of distinct clusters are highlighted in Figure 1, including two regions within the topology that are manifest as a ~50 year recurring cluster containing 20 unique events.

We quantify the patterns evident in these topological representations using statistical scores in Table S1. In topological networks defined using date alone, many sets of events are also distinct with respect to renewal interval, implying that event timing is correlated to renewal interval. For example, the group of events mapped using only timing properties that contains the longest renewal interval event is statistically distinct from the remainder of the catalog with respect to renewal interval with a Kolmogorov-Smirnov (KS) score of 0.91, even though renewal interval is not used as a parameter for the lenses. In the topological network created using both date and renewal interval (Figure 1), the most distinct clusters have high KS scores for both parameters, typically 0.7–0.9 (Table S1), a pattern which persists using a subset of events occurring from 1917 to 2017 (Figure S4 and Table S2), or stochastically decimated catalogs (Figure S7 and Table S2). Truncating the catalog at higher magnitudes yields different topologies, mainly as a consequence of the large decrease in event number (Figures S5 and S6) from 1689 to 449 and then 83 with cutoffs at $M \geq 7.5$ and $M \geq 8.0$, respectively. In contrast, for catalogs with randomized event timing, clusters in topological networks based on date alone have low KS scores for renewal interval, and topological networks created using both date and renewal intervals contain a particular absence of clusters with statistically tight ranges of both dates and renewal intervals (Figure S2 and Table S1).

In a second analysis method, we examine the interevent-interval between all pairs of $M_w \geq 7$ earthquakes (1900–2015) independent of magnitude and location and including aftershocks (Figure 3). We calculate >1.5 million interevent intervals, the time in years separating every possible pair of earthquakes in the catalog and discard noncausal negative intervals. A histogram of 1 year bins derived from these intervals describes an approximately linear relationship with intercept $26,155 \pm 75$ and slope -228.1 ± 1.1 per year. The residual from this straight line (fit in a least squares sense), however, shows a 32.4 ± 1 year period quite unlike that calculated in multiple iterations of random numbers. This approximate periodicity was noted also by Bragato and Segan [2014], and its presence is sufficiently clear for it to be discerned in a simple autocorrelation of the earthquake count time series. Aftershocks and foreshocks empirically eliminated in the “declustered” catalogs of other studies [Shearer and Stark, 2012] are readily identified as a peak at zero to 6 years (Figure 2b).

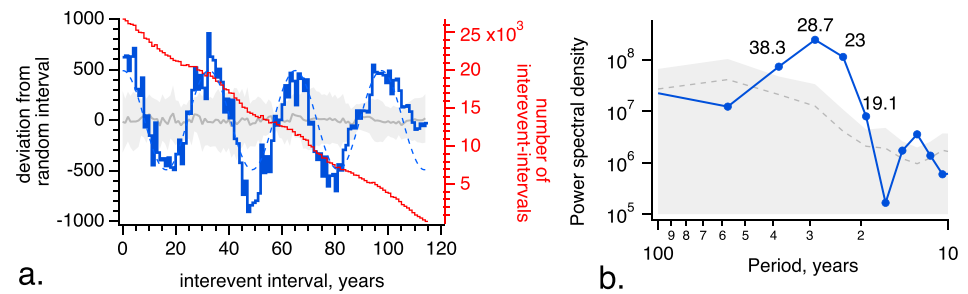


Figure 3. (a) Deviation of interevent-intervals in the $M_w > 7$ global 1900–2015 earthquake catalog (blue trace) compared to random catalogs with identical numbers of events and duration (grey). Red trace shows the histogram of interevent intervals from which the residual from a least squares fit is obtained. Peaks in the earthquake catalog exceed the standard deviation in the random data by a factor of 2 with a cyclic period of 32.4 ± 2 years (dashed blue sine wave). The peak in short renewal intervals (< 6 years) represent aftershocks and foreshocks that we have not removed from the catalog. (b) Spectral peaks with periods between 20 and 40 years in the residual $M_w > 7$ earthquake catalog (blue trace) rise almost an order of magnitude above the mean and standard deviation of stacked power spectra (grey) derived from random catalogs.

Although the numbers of interevent intervals are similar at all the peaks, the percentages of earthquakes with interevent intervals of ≈ 32 , ≈ 64 , and ≈ 99 years exceeds the total number of interevent intervals at these periods by 2.5%, 1.5%, and 10%, respectively. To test for the significance of the observed peaks, we generated 30 random catalogs with 1740 dates randomly selected using a Mersenne-Twister algorithm. No significant change in the standard deviation of the residuals from the linear fits to the random histograms occurred after 20 iterations. Least squares fits to these histograms yield a mean intercept 26204 ± 236 and slope -228.6 ± 0.3 , similar to the natural catalog, but the unexpected periodicity in interevent times in the natural earthquake catalog exceeds that of the random data by 2 standard deviations.

A power spectral analysis shows its spectral density to be broader than suggested by the sine wave fit, but the amplitude of its dominant period of ≈ 32 years exceeds those derived from spectral analyses of synthetic random-number catalogs by an order of magnitude. This 32 year interevent interval is unexpected and again suggests that the timing of global earthquakes is not random. The spectra in Figure 3b were obtained using a fast Fourier transform padded from 115 to 128 samples tapered with a Hanning window.

4. Discussion

The underlying mechanical coupling required for synchronization arises from the elastic properties of the solid earth. These properties allow both dynamic and static strain related to the loading and rupture of the earthquake “cycle” to be expressed over hemispheric length scales; this strain suffices to organize events with similar renewal intervals into quasi-periodic noisy clusters. Other sources of global strain can also excite organization of sets of events with appropriate renewal intervals. For example, finite strain with notable periodicity appears to result from the partition of angular momentum between the solid earth and its fluid layers [Gross *et al.*, 2004]. The influence of such planetary-scale coupling has previously been recognized as statistical structure in the earthquake catalog [Ferreira *et al.*, 2014], and through the relationship of external forcing to earthquake occurrence [e.g., Scholz, 2010], with the capacity of weakly coupled oscillators to synchronize dependent on the nature of the coupling, the intensity of forcing, and the distribution of renewal intervals [e.g., Sammis and Smith, 2013], complicated by inelastic effects, direct triggering, renewal variability, and the capacity of faults to host events of many magnitudes on the same domain. Rotational accelerations of the Earth correspond to peaks in global seismic productivity [Anderson, 1974; Varga *et al.*, 2012; Shanker *et al.*, 2001] (Figure 4a). These decadal rotational fluctuations are irregular, with broad rotational and earthquake maxima evident at 33, 60, and 88 year intervals, accompanied by minor intervening peaks. We envisage that these multidecadal periods provide a rich spectrum for stimulating synchronization, with periods particularly close to the renewal interval of many circum-Pacific events, hence well suited to exciting synchronized sets. Gathering of groups of earthquakes into phase alignment can be excited by static [Press, 1965] and dynamic [Agnew and Wyatt, 2014] strains propagating to great distances (Figure 4b) or combinations thereof.

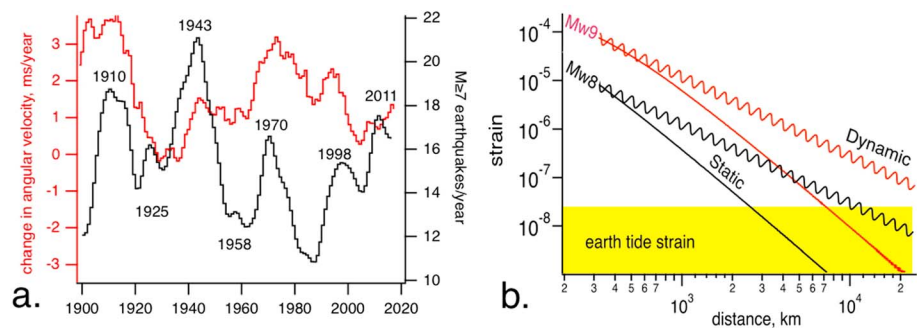


Figure 4. (a) Changes in the length of the day [Gross *et al.*, 2004] correlate with decadal fluctuations in annual $M \geq 7$ earthquakes [Anderson, 1974; Shanker *et al.*, 2001] (smoothed with 10 year running mean). Peak seismic activity and rotational acceleration occur at 15, 33, 60, and 88 year intervals. (b) Static [Press, 1965] and dynamic [Agnew and Wyatt, 2014] strain from distant $M_w = 8$ and $M_w = 9$ earthquakes exceed earth tide strain amplitudes at distances of 2500–30,000 km. Distances between plate boundaries are typically 1000–12,000 km; hence, the largest of Earth's earthquakes provides the weak force required for hemispheric synchronization.

Synchronization differs from direct forcing in that it requires many cycles for alignment, and the forces acting on the ensemble may be extremely small [e.g., Oliveira and Melo, 2015]. Once developed, phase-aligned events with similar renewal intervals are then likely to remain in phase over many cycles, either growing in number of members or remaining stable if coupling attenuates with distance [Leyva *et al.*, 2011]. However, because faults are imperfect oscillators and the system of faults on Earth is subject to a diverse set of both elastic and inelastic forcing, we do not expect either individual faults or event clusters to repeat in perfect cycles, hence the longstanding observation that event recurrence intervals on single faults and systems of faults [Dietrich, 1992; Barbot *et al.*, 2012] are highly irregular. So, therefore, should cluster synchronization be statistically quantifiable but not necessarily directly observable as repeat identical event sets on systems of faults? The paucity of repeat clusters containing identical events in Figure 1 is exacerbated by our method of calculating renewal intervals which, because of uncertainties in characteristic scaling, tectonic velocities, and plate boundary coupling, provides values which are internally consistent and likely to be proportional to the real values but are unlikely to be exactly correct for the events cataloged.

The patterns described are anticipated from the general properties of synchronization of physical oscillators subject to weak interaction. Although indications of earthquake clustering have been identified in some previous studies [Corral, 2004; Davidsen *et al.*, 2006; Scholz, 2010] and discounted as random by others [e.g. Ben-Naim *et al.*, 2013; Beroza, 2012], the presence of temporal clustering of earthquakes with common renewal interval suggests synchronization may arise from the nonlinear properties of integrate-and-fire (or any other) oscillators, thus revealing both a temporal structure and a physical mechanism distinct from the case when earthquakes are considered as events with no oscillatory properties. However, other properties of the earthquake cycle still preclude exactly repeating clusters by disrupting synchronization, especially viscous dissipation of earthquake-induced stress changes [Scholz, 2010; Sammis and Smith, 2013], as well as theoretically predicted excursions from synchronization by individual oscillators when their periods are not identical, noisy, or perturbed by external forcing [Pikovsky *et al.*, 2003]. Global seismic synchronization has no utility for the precise prediction (in a strict sense) of specific damaging earthquakes, but these results do imply that the probability of events is time dependent. Thus, earthquakes with a certain renewal interval are more likely to occur when similar renewal interval earthquakes have recently occurred, or at times corresponding to maxima in Earth's rotational deceleration or acceleration.

Acknowledgments

All of the data used in this study are already available through open sources. We are grateful to Ayasdi, Inc., for allowing use of their software for research purposes and to two anonymous reviewers. We also thank Walter Szeliga and Kristy Tiampo for insightful discussions and suggestions.

References

- Acebron, J., L. Bonilla, S. DeLeo, and R. Spigler (1998), Breaking the symmetry in bimodal frequency distributions of globally coupled oscillators, *Phys. Rev. E*, *57*, 5287–5290.
- Agnew, D. C., and F. K. Wyatt (2014), Dynamic strains at regional and teleseismic distances, *Bull. Seismol. Soc. Am.*, *104*, 41,846–41,859.
- Anderson, D. L. (1974), Earthquakes and the Rotation of the Earth, *Science*, *186*, 49–50, doi:10.1126/science.186.4158.49.
- Barbot, S., N. Lapusta, and J.-P. Avouac (2012), Under the hood of the earthquake machine: Toward predictive modeling of the seismic cycle, *Science*, *336*, 707–710, doi:10.1126/science.1218796.
- Ben-Naim, E., E. Daub, and P. Johnson (2013), Recurrence statistics of great earthquakes, *Geophys. Res. Lett.*, *40*, 3021–3025, doi:10.1002/grl.50605.

- Beroza, G. (2012), How many great earthquakes should we expect?, *Proc. Natl. Acad. Sci. U.S.A.*, *109*, 651–652, doi:10.1073/pnas.1120744109.
- Berryman, K., et al. (2015), The GEM faulted earth subduction interface characterization project, Version 2.0, April 2015, GEM Faulted Earth Project. [Available from <http://www.nexus.globalquakemodel.org/gem-faulted-earth/post.s.>]
- Bragato, P. L., and M. Sagan (2014), Decreasing rate of $M \geq 7$ earthquakes in the northern hemisphere since 1900, *Seismol. Res. Lett.*, *85*(6), 1–9, doi:10.1785/0220140111.
- Calais, E., T. Camelbeeck, S. Stein, M. Liu, and T. Craig (2016), A new paradigm for large earthquakes in stable continental plate interiors, *Geophys. Res. Lett.*, *43*, 10–637, doi:10.1002/2016GL070815.
- Carlsson, G. (2009), Topology and data, *Bull. Am. Math. Soc.*, *46*, 255–308.
- Corral, A. (2004), Long-term clustering, scaling, and universality in the temporal occurrence of earthquakes, *Phys. Rev. Lett.*, *92*, 108501.
- Czolczynski, K., P. Perlikowski, A. Stefanski, and T. Kapitaniak (2009), Clustering and synchronization of n Huygens' clocks, *Phys. A: Stat. Mech. Appl.*, *388*, 5013–5023, doi:10.1016/j.physa.2009.08.033.
- Daido, H. (1995), Multi-branch entrainment and multi-peaked order-function in a phase model of limit-cycle oscillators with uniform all-to-all coupling, *J. Phys. A Math. Gen.*, *28*, L151–L157.
- Daub, E., D. Trugman, and P. Johnson (2015), Statistical tests on clustered global earthquake catalogs, *J. Geophys. Res. Solid Earth*, *120*, 5693–5716, doi:10.1002/2014JB011777.
- Davidson, J., P. Grassberger, and M. Paczuski (2006), Earthquake recurrence as a record breaking process, *Geophys. Res. Lett.*, *33*, L11304, doi:10.1029/2006GL026122.
- Dietrich, J. (1992), Earthquake nucleation on faults with rate- and state-dependent strength, *Tectonophysics*, *211*, 115–134.
- DiGiacomo, D., J. Harris, A. Villasenor, D. Storchak, R. Engdahl, W. Lee, and the Data Entry Team (2015), ISC-GEM: Global instrumental earthquake catalogue (1900–2009), I. Data collection from early instrumental seismological bulletins, *Phys. Earth Planet. Inter.*, *239*, 14–24, doi:10.1016/j.pepi.2014.06.003.
- Engdahl, E., and A. Villasenor (2002), Global seismicity: 1900–1999, in *International Handbook of Earthquake and Engineering Seismology*, vol. 81A, edited by W. H. K. Lee et al., pp 665–690, Academic Press, San Diego, Calif.
- Ferreira, D. S., A. R. Papa, and R. Menezes (2014), Small world picture of worldwide seismic events, *Phys. A: Stat. Mech. Appl.*, *408*, 170–180.
- Gross, R. S., I. Fukumori, D. Menemenlis, and P. Goutou (2004), Atmospheric and oceanic excitation of length-of-day variations during 1980–2000, *J. Geophys. Res.*, *109*, B01406, doi:10.1029/2003JB002432.
- Kuramoto, Y. (1975), Self-entrainment of a population of coupled nonlinear oscillators, in *Lecture Notes in Physics*, vol. 39, edited by H. Aoki, pp. 420–422, Springer, Berlin Heidelberg.
- Kuramoto, Y., and Battogtokh, D. (2002), Coexistence of coherence and incoherence in nonlocally coupled phase oscillators. *arXiv preprint cond-mat/0210694*.
- Leonard, M. (2010), Earthquake fault scaling: Self-consistent relating of rupture length, width, average displacement, and moment release, *Bull. Seismol. Soc. Am.*, *100*, 1971–1988, doi:10.1785/0120090189.
- Leyva, I., A. Navas, I. Sendina-Nadal, J. Buldu, J. Almendral, and S. Boccaletti (2011), Synchronization waves in geometric networks, *Phys. Rev. E*, *84*, 065101.
- Lum, P., G. Singh, A. Lehman, T. Ishkanov, M. Vejdemo-Johansson, M. Alagappan, J. Carlsson, and G. Carlsson (2013), Extracting insights from the shape of complex data using topology, *Nat. Sci. Rep.*, *3*, 1236, doi:10.1038/srep01236.
- Michael, A. (2014), How complete is the ISC-GEM global earthquake catalog?, *Bull. Seismol. Soc. Am.*, *104*, 1829–1837.
- Mirollo, R., and S. Strogatz (1990), Synchronization of pulse-coupled biological oscillators, *SIAM J. Appl. Path.*, *50*, 1645–1662.
- Okuda, K. (1993), Variety and generality of clustering in globally coupled oscillators, *Phys. D*, *63*, 424–436.
- Oliveira, H. M., and L. V. Melo (2015), Huygens synchronization of two clocks, *Sci Rep*, *5*.
- Pikovsky, A., M. Rosenblum, and J. Kurths (2003), *Synchronization: A Universal Concept in Nonlinear Sciences*, 411 pp., Cambridge Univ. Press, Cambridge.
- Press, F. (1965), Displacements, strains, and tilts at teleseismic distances, *J. Geophys. Res.*, *70*, 2395–2412, doi:10.1029/JZ070i010p02395.
- Prignano, L., O. Sagarra, P. M. Gleiser, and A. Diaz-Guilera (2012), Synchronization of moving integrate and fire oscillators, *Int. J. Bifurcation Chaos*, *22*, 1250179.
- Reasenburg, P. (1985), Second-order moment of Central California seismicity, 1969–1982, *J. Geophys. Res.*, *90*, 5479–5495, doi:10.1029/JB090iB07p05479.
- Rundle, J., K. Tiampo, W. Klein, and J. Sa Martins (2002), Self-organization in leaky threshold systems: The influence of near-mean field dynamics and its implications for earthquakes, neurobiology, and forecasting, *Proc. Natl. Acad. Sci. U.S.A.*, *99*, 2514–2521.
- Sammis, C., and S. Smith (2013), Triggered tremor, phase-locking, and the global clustering of great earthquakes, *Tectonophysics*, *589*, 167–171.
- Scholz, C. (2010), Large earthquake triggering, clustering, and the synchronization of faults, *Bull. Seismol. Soc. Am.*, *100*, 901–909, doi:10.1785/0120090309.
- Scholz, C., and J. Campos (2012), The seismic coupling of subduction zones revisited, *J. Geophys. Res.*, *117*, B05310, doi:10.1029/2011JB009003.
- Sella, G. F., T. H. Dixon, and A. Mao (2002), REVEL: A model for recent plate velocities from space geodesy, *J. Geophys. Res.*, *107*(B4), 2081, doi:10.1029/2000JB000033.
- Shanker, D., N. Kapur, and V. Singh (2001), On the spatio temporal distribution of global seismicity and rotation of the earth—A review, *Acta Geod. Geoph. Hung.*, *36*, 175–187.
- Shearer, P. M., and P. B. Stark (2012), Global risk of big earthquakes has not recently increased, *Proc. Natl. Acad. Sci. U.S.A.*, *109*, 717–721.
- Singh, G., F. Memoli, and G. Carlsson (2007), Topological Methods for the Analysis of High Dimensional Data Sets and 3D Object Recognition, in *Eurographics Symposium on Point Based Graphics*, European Association for Computer Graphics, pp. 91–100.
- Varga, P., F. Krumm, F. Riguzzi, C. Doglioni, B. Sule, K. Wang, and G. Panza (2012), Global pattern of earthquakes and seismic energy distributions: Insights for the mechanisms of plate tectonics, *Tectonophysics*, *530*, 80–86.
- Wang, W., I. Kiss, and J. Hudson (2000), Experiments on arrays of globally coupled chaotic electrochemical oscillators: Synchronization and clustering, *Chaos*, *10*, 248–256.
- Winfree, A. (1967), Biological rhythms and the behavior of populations of coupled oscillators, *J. Theoret. Biol.*, *16*, 15–42.